A Short Autocomplementary Sequence in the 5′ Leader Region Is Responsible for Dimerization of MoMuLV Genomic RNA†

Pierre-Marie Girard, Bénédicte Bonnet-Mathonière, Delphine Muriaux, and Jacques Paoletti*

Unité de Biochimie, URA 147 CNRS, rue Camille Desmoulins, Institut Gustave Roussy, 94805 Villejuif, France

Received January 6, 1995; Revised Manuscript Received May 26, 1995⊗

ABSTRACT: Previous work has shown that a region of Moloney murine leukemia virus (MoMuLV) RNA located between nucleotides 280 and 330 in the PSI region (nt 215−565) is implicated in the dimerization process. We show with a deletion from nucleotides 290−299 in PSI RNA transcripts and through an antisense oligonucleotide complementary to nucleotides 275−291 that the 283−298 region is involved in RNA dimer formation *in vitro*. In an attempt to further characterize the mechanism of dimer formation, a series of short RNA transcripts was synthesized which overlapps the PSI region of MoMuLV RNA. The dimerization of these RNAs is temperature dependent. The predicted secondary structure of the 278−303 region, as a function of temperature, reveals that this sequence is able to adopt two conformations: (1) the $U^{288}AGCUA^{293}$ sequence in a loop; (2) part of the same nucleotides implicated in a stem. These results, together with thermodynamic analysis, strongly suggest that (1) the loop conformation of the UAGCUA sequence modulates the relative amount of RNA dimer and (2) a 16 bp long Watson−Crick base pairing is involved in RNA dimer formation. We propose that loop−loop recognition *via* the $U^{288}AGCUA^{293}$ sequence leads to a stable structure induced by a stem−loop opening. Furthermore, our results do not support purine quartet formation as necessary for the dimerization of the 5′ leader MoMuLV RNA.

All known retroviral genomes are packaged into particles as a dimer of identical RNA molecules, and it has been postulated that dimer formation is closely related to encapsidation (Bieth et al., 1990; Darlix et al., 1990; Prats et al., 1990). The location of the packaging signal has been characterized for various retroviral species [Aldovini & Young, 1990; Katz et al., 1986; Lever et al., 1989; Mann et al., 1983; Stocker & Bissel, 1979; Watanabe & Temin, 1982; for a review, see Rein (1994)], and appears to depend on a cis-acting element called PSI. PSI normally maps in the 5′-terminal noncoding region of viral genome, but can extend to other regions (Aronoff & Linial, 1991; Adam & Miller, 1988; Armentao et al., 1987; Bender et al., 1987; Linial & Miller, 1990; Murphy & Goff, 1989). Retroviral RNA genomes are joined together by a dimer linkage structure (DLS)[1] which apparently leads to parallel (5′−5′) linkage, as shown through electron microscopy studies of partially denatured dimer molecules (Bender & Davidson, 1976; Bender et al., 1978; Kung et al., 1976; Murti et al., 1981). The DLS has been mapped within the PSI region in MoMuLV (Mann et al., 1983; Mann & Baltimore, 1985; Prats et al., 1990). These data support the hypothesis that dimerization and encapsidation are related processes and that the dimer linkage structure is part of the signal for the encapsidation of unspliced retroviral RNA. It has also been suggested that dimerization is associated with reverse transcription through interstrand switching (Luo & Taylor, 1990; Panganibam & Fiore, 1988; Temin, 1991), genomic recombination (Hu & Temin, 1990; Weiss et al., 1973), and inhibition of translation (Bieth et al., 1990). This physical interaction between two retroviral RNA molecules is important for a normal viral cycle.

Dimerization of retroviral RNA can occur spontaneously *in vitro* (Bieth et al., 1990; Darlix et al., 1990; Prats et al., 1990; Roy et al., 1990), implying direct interactions between two RNA molecules, although it is highly stimulated by nucleocapsid protein (Bieth et al., 1990; Darlix et al., 1990; Prats et al., 1988, 1990).

Models for dimer formation were deduced from potential base pairing within the 5′ leader sequence of the viral genome (Coffin, 1984; Haseltine et al., 1977). More recent studies support a model based on an unusual conformation containing PuGGAPuA sequences which may form four-stranded structures (Awang & Sen, 1993; Marquet et al., 1991; Sundquist & Heaphy, 1993; Torrent et al., 1994).

In a previous work, it has been shown that an RNA transcript (PSI RNA) corresponding to nt 215−565 can efficiently dimerize under defined salt (i.e., Na^+ and Mg^{2+}) and RNA concentrations as well as temperature (Roy et al., 1990). In this work, it has been concluded that (1) due to the very slow rate of the reaction M + M → D, dimer formation probably depends upon a conformational change in the monomeric RNA structure, and (2) at least 10−15 nucleotides in a single stretch are associated within the dimer through canonical base pairing (Roy et al., 1990). Furthermore, Prats et al. (1990) suggested that the DLS probably maps between positions 280 and 330 from the RNA 5′ end. Finally, Tounekti et al. (1992) investigated the conformation

† This work was supported by the Agence Nationale de la Recherche sur le SIDA (ANRS). D.M., a student at the Institut de Formation Supérieure Biomédicale (IFSBM), is supported by a Synthélabo fellowship.

* To whom correspondence should be addressed.

⊗ Abstract published in *Advance ACS Abstracts,* July 15, 1995.

[1] Abbreviations: DLS, dimer linkage structure; HIV-$1_{MAL(or\ LAI\ or\ HXB2)}$, human immunodeficiency virus type-1 MAL (or LAI or HXB2) strain; HIV-2_{ROD}, human immunodeficiency virus type-2 ROD strain; MoMuLV, Moloney murine leukemia virus; Pu, purine; nt, nucleotide(s); TCA, trichloroacetic acid.

0006-2960/95/0434-9785$09.00/0

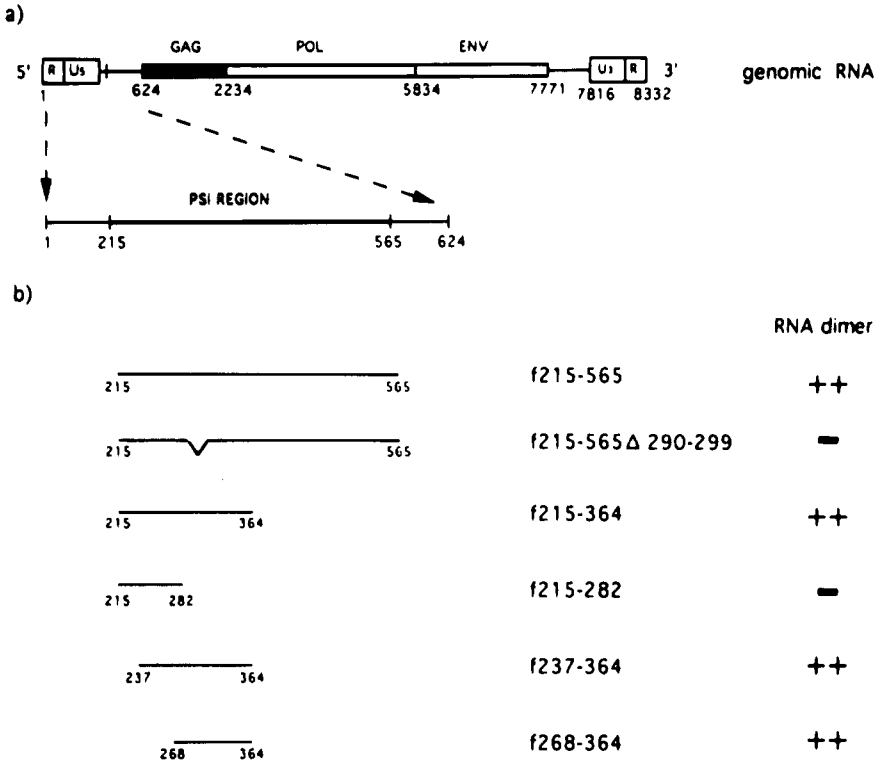

FIGURE 1: Mapping of the sequence necessary for MoMuLV RNA dimerization. (a) Region of the packaging signal sequence (PSI) inside the genomic RNA. Numbering is in relation to the cap site (+1). (b) MoMuLV RNA used in the present work and synthetized *in vitro* (details of construction are given under Materials and Methods). The symbol Δ indicates a deletion spanning nucleotides 290−299. The column headed RNA dimer indicates the maximum level of dimeric RNA observed in buffer D100 and at 50 °C. (−) 0−10%; (++) 70−90%.

of PSI RNA in solution by chemical probing and presented evidence that PSI RNA forms a highly structured domain. In particular, these authors showed that (1) the putative DLS defined by Prats et al. (1990) (positions 280 and 330) is part of two stem−loop structures (one corresponding to nt 278−309 and the other to nt 310−352), and (2) dimerization induces an extensive reduction of reactivity in region 278−309 that can be interpreted as the result of intermolecular interactions and/or intramolecular conformational rearrangements (Tounekti et al., 1992). It is noteworthy that this particular region bears a perfect autocomplementary sequence spanning nucleotides 283−298 (Shinnick et al., 1981).

In the present work, we show by deletion and use of antisense oligonucleotide that part of sequence 278−309 is implicated in RNA dimer formation. Taking into account the predictive secondary structure of this sequence as a function of temperature and our experimental data, we suggest that a conformational rearrangement of sequence 278−309, in the monomer, is triggering the dimerization process. Thermodynamic analysis of the dimerization *in vitro* could reflect Watson−Crick base pairing, and our data allow us to propose a model of RNA−RNA interaction based upon loop−loop recognition.

MATERIALS AND METHODS

Plasmid Construction and Digestion. Standard procedures and sequencing were used for restriction enzyme digestion and plasmid construction (Sambrook et al., 1989). *Escherichia coli* DH5α was used for plasmid amplification. Details of the constructions are given below.

RNA Transcripts 215−282, 215−364, and 215−565. The plasmid pCR2 (Roy et al., 1990) was linearized with the restriction endonuclease *Spe*I, *Bsa*HI, or *Hin*dIII and transcribed with T7 RNA polymerase, giving rise to transcripts starting from position 215 of the MoMuLV RNA sequence and ending at positions 282, 364, and 565. These fragments will be referred to as f215−282, f215−364, and f215−565 (or RNA PSI) (Figure 1). The non-MoMuLV sequence GGGCGAAUUCGAGCUCGCCC is present at the 5′ end of each of these transcripts.

RNA Transcripts 237−364 and 268−364. Polymerase chain reaction was performed on pCR2 with two sets of oligonucleotides: the first set contained oligonucleotide O1, carrying a *Bam*HI site and 16 nucleotides corresponding to the complementary part of positions +364 (5′) to +349 (3′) of the MoMuLV genome, and oligonucleotide O2 corresponding to nt +237 (5′) to +261(3′). The second set contained oligonucleotide O1 and oligonucleotide O3, which corresponds to positions +268 (5′) to +282 (3′). The amplified products were purified, digested with *Bam*HI, and ligated between the *Eco*RI site that was blunted using S1 nuclease and the *Bam*HI site of pGEM3ZF(−), thus generating two plasmids: p237−364 and p268−364. The *Bam*HI linearized plasmids were transcribed, giving rise to f237−364 and f268−364 (Figure 1). The non-MoMuLV sequence GGGCG is present at the 5′ end of f237−364 and f268−364.

RNA Transcripts 215−565Δ290−299. Polymerase chain reaction was performed on pCR2 with 5′CCTGCGTCGGTACTAGTTATCTGTATCTGGCGGACC3′ oligonucleotide, which corresponds to nt 271 (5′) to 316 (3′) and lacks nucleotides 290 through 299 of the MoMuLV genome, and T3 universal primer. The polymerase chain reaction product was digested by *Spe*I and *Hin*dIII. The DNA fragment

corresponding to nt 215−282 was prepared by digestion of pCR2 by *Eco*RI and *Spe*I. Both fragments were purified and ligated between the *Eco*RI and *Hin*dIII sites of pGEM3ZF-(−), thus generating pPSIΔ290−299. After linearization at the *Hin*dIII site, this plasmid was transcribed and gave rise to fPSIΔ290−299 (Figure 1). The non-MoMuLV sequence GGGCGAAUUCGAGCUCGCCC is present at the 5′ end of this transcript.

In Vitro RNA Synthesis and Purification. Five micrograms of linearized plasmids was transcribed using 4 μL of T7 RNA polymerase (Gibco-BRL, 50 units/μL) in 40 mM Tris-HCl, pH 8, 20 mM $MgCl_2$, 5 mM DTT, 1 mM spermidine, 0.01% Triton X-100, 0.01 mg/mL BSA, and 5 mM each of rXTP in the presence of 40 units of RNasin (Promega) in 0.1 mL final volume. After treatment with DNaseI−RNase free (Boehringer-Mannheim), the RNA transcripts were phenol/chloroform extracted and ethanol precipitated. The precipitate was dissolved in sterile double-distilled water (80 μL) and twice precipitated with lithium perchlorate in 500 μL of acetone. After centrifugation, the transcripts were resuspended in 50 μL of sterile water and microdialyzed (Millipore filters type V6, 0.025 μm) for 2 h against sterile double-distilled water. The purity and integrity of the RNAs were checked on polyacrylamide gel electrophoresis in denaturing conditions, and the concentration was determined by UV spectroscopic measurement at 260 nm.

In Vitro Dimerization. In a standard experiment, RNA, in 8 μL of MiIlli-Q (Millipore) water, was heated for 2 min at 90 °C, chilled on ice for 2 min, and adjusted to 10 μL with 2 μL of 5-fold concentrated buffer (buffer D100 5x = 500 mM NaCl, 250 mM Tris-HCl, pH 7). The samples were incubated for 0−240 min at temperatures ranging from 4 to 65 °C (for temperatures higher than 30 °C, mineral oil was added in order to prevent evaporation). Incubation was conducted in 50 mM Tris-HCl, pH 7, 100 mM NaCl, and 0.8 μM RNA strand concentration.

At the end of incubation, all the samples were cooled on ice, mixed with 2 μL of loading buffer (50% w/v glycerol and 0.025% w/v tracking dyes), loaded on a 1.5% Seakem or 2% Seakem-2% (w/v) Nusieve agarose gel, and electrophoresed at 5 V/cm and 4 °C in buffer containing 50 mM Tris−borate, pH 8.3, 1 mM EDTA, and 0.2 μg/mL ethidium bromide.

The ^{32}P-labeled DNA (1 μL per tube) with unlabeled oligonucleotides (at an oligonucleotide/RNA ratio of 1/1 or 5/1) was annealed by adding DNA oligomers to RNA prior to heating for 2 min at 90 °C. The agarose gel was first stained with ethidium bromide to analyze the unlabeled RNA and then fixed in 5% TCA, dried, and autoradiographed to analyze oligonucleotide annealing.

Gels were scanned for fluorescence by Bioprofil (Vilber-Lourmat France), and the peak surface was integrated. The percent of dimer was derived by calculating the ratio between the surfaces of the peaks corresponding to the dimer and the sum of peak surfaces corresponding to dimer and monomer. The rate constant of the reaction and the relative percent of dimer formed at equilibrium were derived assuming a simple bimolecular reaction and solving the integrated form of the equation (Moor & Pearson, 1981).

Melting Temperature Determination of Dimer Dissociation. RNA transcripts, at a final strand concentration of 10 μM in water, were heated to 90 °C for 2 min and chilled on ice for 2 min. Buffer D100 was added, as above, and the RNA solutions were incubated for 90 min at the predetermined optimal temperature for complete dimerization. The resulting dimer was then microdialyzed (Millipore filters type V6, 0.025 μm) for 2 h at 4 °C against 50 mM Tris-HCl, pH 7.5, 100 mM NaCl, and 1 mM EDTA. If necessary, the samples were diluted in the same buffer in order to obtain concentrations ranging from 0.1 μM to 2 μM RNA strand concentration. The effect of salt concentrations on the thermal stability of RNA dimer was investigated with NaCl concentrations ranging from 50 mM to 300 mM for an RNA strand concentration of 0.8 μM. Aliquots (10−20 μL) of each sample were then incubated for 5 min at temperatures ranging from 4 to 80 °C and electrophoresed as described above. After ethidium bromide staining and fluorescent scanning of the gels, the percentages of dimer and monomer were estimated. The thermal melting temperature (T_m) of the reaction D ↔ M + M was estimated from the plot of the amount of dimer as a function of temperature. $\Delta H°$ and $\Delta S°$ for the dissociation were then derived by fitting the curve to a two-state model (Petersheim & Turner, 1983) from the equation: $1/T_M = (R/\Delta H°) \ln C_t + \Delta S°/\Delta H°$, where C_t is the total RNA strand concentration and $\Delta H°$ and $\Delta S°$ are the enthalpic and entropic parameters, respectively.

Antisense DNA Oligomer. Oligonucleotides OL275−291 and OL268−282, complementary to MoMuLV RNA at positions 275−291 and 268−282, respectively, were synthesized (Bioprobe System), 5′ end-labeled with [γ-^{32}P]ATP, using T4 polynucleotide kinase (Boehringer-Mannheim), and purified on a 15% denaturing polyacrylamide gel in 89 mM Tris−borate, 2 mM EDTA. End-labeled oligonucleotides were redissolved in sterile double-distilled water at 50 × 10^3cpm/μL.

RESULTS

Inhibition of Dimerization by Complementary Oligonucleotide. Two antisense oligonucleotides were synthesized: OL275−291, which is complementary to nt 275−291, and OL268−282, which is complementary to nt 268−282 of MoMuLV genomic RNA. Each oligonucleotide was incubated with f215−565, f215−364, f237−364, and f268−364 in buffer D100 for an oligonucleotide/RNA ratio of 1/1 or 5/1. The effect of oligonucleotide hybridization on dimerization kinetics was tested at 50 °C. As shown in Figure 2, OL268−282 had no effect on the dimerization of f215−565 and f268−364 RNAs, even for an oligonucleotide/RNA ratio of 5/1. An excess of oligonucleotide OL268−282 slightly inhibited the dimerization of f215−364 and f237−364. In contrast, oligonucleotide OL275−291 had a strong effect on RNA dimerization. At an oligonucleotide/RNA ratio of 1/1, the inhibition of RNA dimerization was about 50% for f215−565, f237−364, and f268−364, and about 75% for f215−364. At an oligonucleotide/RNA ratio of 5/1, no more than 10% of the RNA was dimeric (Figure 2). Using ^{32}P end-labeled oligonucleotide, we found that OL268−282 anneals to both monomeric and dimeric RNA whereas OL275−291 anneals only to monomeric RNAs f215−565, f215−364, f237−364, and f268−364 (data not shown).

Deletion inside f215−565. These above results show that sequence 268−282 is not implicated in RNA dimer formation and that all or part of nucleotides from 283 to 291 should participate in the RNA−RNA interaction. Accordingly, we examined the effect of deletion inside the 283−298 auto-

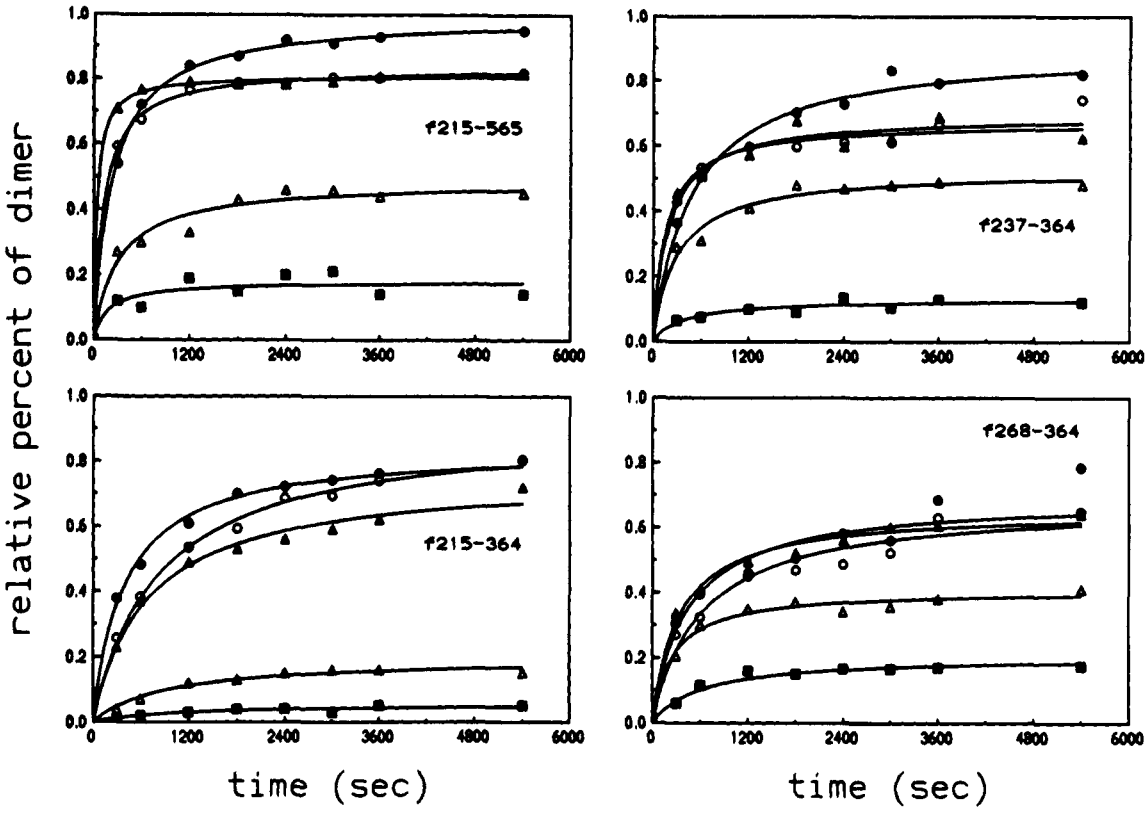

FIGURE 2: Kinetics of dimerization of f215−565, f215−364, f237−364, and f268−364 without (●) or with oligonucleotide OL268−282 (○, ▲) or oligonucleotide OL275−291 (△, ■) at an oligonucleotide/RNA ratio of 1/1 (○, △) or 5/1 (▲, ■) in buffer D100 and at 50 °C.

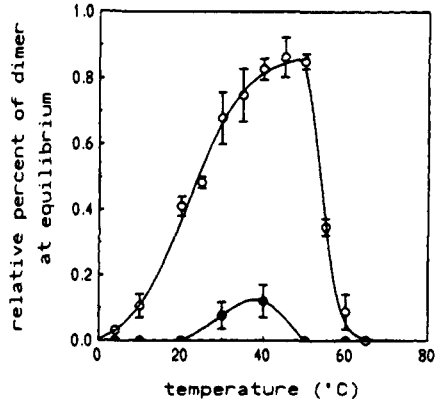

FIGURE 3: Amount of dimer formed at equilibrium as a function of temperature for f215−565 (○) and f215−565Δ290−299 (●). Δ symbolizes deletion of nt 290−299. Experimental conditions are 50 mM Tris-HCl, pH 7, 100 mM NaCl. The total RNA strand concentration is 0.8 μM.

complementary region. Taking into account the secondary structure of the PSI region determined in solution by chemical probing (Tounekti et al., 1992), a deletion spanning nucleotides 290−299 was created in f215−565. The RNA transcript 215−565Δ290−299 (Materials and Methods) was tested for its ability to dimerize in buffer D100 and between 4 and 65 °C. As shown in Figure 3, f215−565Δ290−299 did not significantly dimerize.

This observation together with the inhibition induced by antisense oligonucleotide supports the hypothesis that the 283−298 sequence is essential for dimerization of RNA. Furthermore, such results imply that the non-MoMuLV sequence present at the 5′ end of each RNA transcript (Materials and Methods) is not involved in the process of dimerization.

The Dimerization Yield Is a Function of Temperature. It has been shown that the PSI region adopts a similar conformation, irrespective of whether it is isolated or part of the 1−725 sequence (Tounekti et al., 1992). Thus, the PSI region can function as an independent domain inducing dimerization (Tounekti et al., 1992).

In an attempt to characterize the dimerization process, we compared the dimerization kinetics of the PSI transcript as already studied (Roy et al., 1990) to the dimerization kinetics of shorter RNA transcripts truncated either at the 5′ and/or at the 3′ end (Figure 1). This could reveal evidence on how sequences within PSI could be implicated in dimerization. In particular, what regions are essential for the induction of dimerization? The short RNA transcripts were incubated at 4−65 °C. RNAs f215−565, f215−364, f237−364 and f268−364, dimerize (Figure 4A, and data not shown for temperatures higher than 50 °C). By scanning the gels, monomeric and dimeric species were quantified, and the relative percent of dimer formed at equilibrium (D_{eq}) and the rate constant (k_1) were derived.

The rate constant and the plateau value depend on the incubation temperature (Figure 4B). The rate constant values reveal that dimerization is a slow process at 10−50 °C (2×10^2 M^{-1} s^{-1} < k_1 < 7×10^3 M^{-1} s^{-1}) (Figure 6) compared to what is usually described for base-pairing of short oligonucleotides or complementary RNAs (k_1 around 10^6−10^7 M^{-1} s^{-1}) (Pörschke et al., 1973; Williams et al., 1989; Grosjean et al., 1976; Labuda & Pörschke, 1980). Thus, the RNA−RNA interaction might not correspond to a pure diffusion model but probably involves conformational changes as rate-limiting steps. Nevertheless, we cannot rule out the implication of non-Watson−Crick base-pairing, as suggested by Marquet et al. (1991).

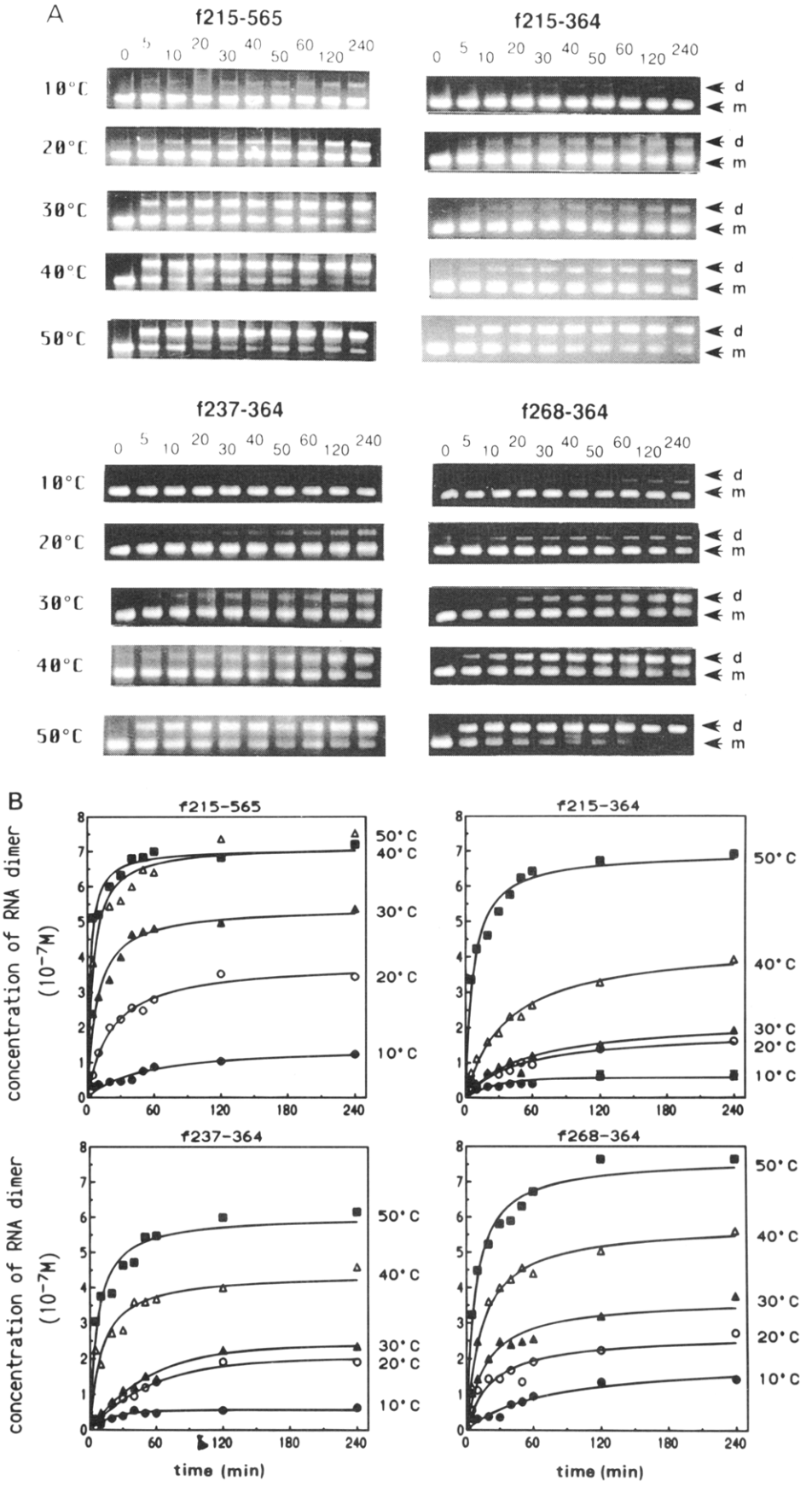

FIGURE 4: Kinetics of dimerization of f215−565, f215−364, f237−364, and f268−364 in buffer D100 for temperatures ranging from 10 to 50 °C. The total RNA strand concentration is 0.8 μM. (A) Ethidium bromide stained agarose gel electrophoresis. m and d indicate monomeric and dimeric RNA, respectively. (B) Concentration of RNA dimer formed as a function of time for temperatures between 10 and 50 °C. (●) 10 °C; (○) 20 °C; (▲) 30 °C; (△) 40 °C; (■) 50 °C. Gels were scanned for fluorescence, and the concentration of each RNA species was calculated as a function of time. The rate constant and the amount of dimer were derived assuming a simple bimolecular reaction and solving the integrated form of the equation (Moore & Pearson, 1981).

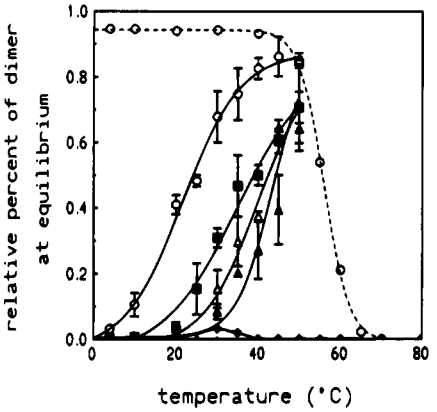

FIGURE 5: Representation of the relative percent of dimer at equilibrium as a function of temperature for f215−565 (○), f215−364 (▲), f237−364 (△), f268−364 (■), and f215−282 (♦). For f215−282, no significant amount of dimer is observed. The experimental points were obtained from the kinetics of dimerization (—) described in Figure 4 and from the thermal stability of the f215−565 dimer (- - -) as described under Materials and Methods. The experimental conditions were as in Figure 3.

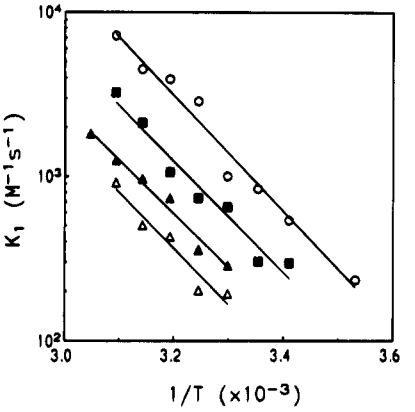

FIGURE 6: Arrhenius plots of the monomer to dimer transition as a function of RNA length. Rate constant values were derived from Figure 4A. f215−565 (○); f215−364 (▲); f237−364 (△); and f268−364 (■). The activation energies are determined by the slope of the rate constant (k_1) as a function of the reciprocal absolute temperature ($1/T$). These values are reported in Table 1.

The dimerization yield, like the rate constant, increases with incubation temperature (Figure 5); 50% of maximal dimerization yield takes place at temperatures <45 °C, e.g., 25 °C for f215−565 to 40 °C for f215−364. The 215−282 transcript did not dimerize, even in the presence of up to 700 mM NaCl or at least 10 mM $MgCl_2$ (not shown). This supports the results drawn from oligonucleotide hybridization and the Δ290−299 deletion.

The lower dimerization yield observed for temperatures >50 °C results from thermally induced destabilization of the dimer. The plot representing thermal dissociation of the dimer can be superimposed on the preceding plot for temperatures from 50 to 80 °C (Figure 5). The variation in dimerization yield at temperatures <45 °C is not related to the stability of the RNA dimers (whose T_m values in these conditions are about 57−60 °C) but is an intrinsic property of the RNA.

In order to elucidate the nature of this variation, we tracked the dimerization of RNA 215−565 at concentrations ranging from 0.1 to 2 μM. The variation was the same for all concentrations studied (not shown), suggesting that dimer formation depends on a thermally induced intramolecular process. Such a change will then promote dimer formation, and the midpoint of the transition represents the temperature at which 50% of the RNA is in a conformation allowing spontaneous dimerization.

Activation Energy of Duplex Formation. Second-order rate constants, determined from the overall process M + M ⟷ D at various temperatures, were used to determine the activation energy (E_a) of monomer to dimer reaction of different RNA lengths. The rate constant of dimer formation (k_1) is connected to E_a by the Arrhenius equation:

$$k_1 = Ae^{-E_a/RT}$$

where A is a "collision factor", R the gas constant, and T the absolute temperature.

To determine the activation energy, the natural logarithm of the measured rate constant was plotted versus reciprocal temperature (Figure 6). The calculated E_a values are reported in Table 1. The slopes of the lines, determined by the Arrhenius equation, are virtually identical, indicating that E_a is not dependent on RNA length. This suggests that the overall process of dimerization is the same whether f215−565, f215−364, f237−364, or f268−364 is considered. Furthermore, the positive values of E_a highly support the idea that the limiting step in RNA dimer formation is not just the intermolecular interactions of complementary sequences (as in duplex formation between two oligonucleotides), but involves also either a conformational rearrangement induced by dimerization itself and/or a conformational rearrangement of the monomer prior to dimerization, or both.

Table 1: Variation of the Activation Energy as a Function of RNA Length for the Overall Process M + M ↔ D[a]

	E_a (kcal/mol)
f215−565	16.1 ± 1.1
f215−364	14.9 ± 1.2
f237−364	15.6 ± 2.4
f268−364	15.5 ± 1.4

[a] The activation energy determined from the Arrhenius equation fit the data in Figure 6.

DISCUSSION

Previous work showed that the PSI region (nt 215−565) efficiently dimerized *in vitro* (Prats et al., 1990; Roy et al., 1990) and that dimer formation was dependent upon RNA, NaCl, and $MgCl_2$ concentrations as well as temperature (Roy et al., 1990). To better understand the structural features involved in MoMuLV RNA dimerization, a series of RNA transcripts including the 5′ noncoding region of MoMuLV genome (Figure 1) was assayed for their ability to dimerize *in vitro*.

A short autocomplementary sequence, from C^{283} to G^{298}, seems essential for this process. When the sequence spanning nucleotides 290−299 was deleted from this region or when an antisense oligonucleotide was hybridized to the 275−291 RNA sequence of MoMuLV, f215−565 was unable to efficiently dimerize. This latter observation supports Prats et al. (1990), who showed that, in the presence of nucleocapsid protein (NCp) (Leis et al., 1988), oligonucleotide complementary to 280−307 nucleotides of MoMuLV inhibited the process of RNA 215−421 dimerization *in vitro*.

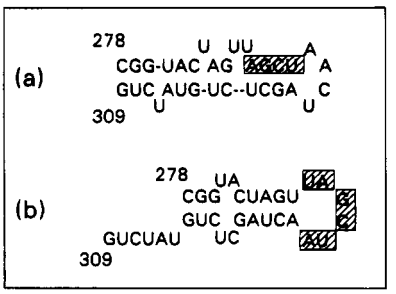

FIGURE 7: Structures of the stem−loop encompassing nucleotides 278−309. These structures to be named 7a and 7b were observed when folding f215−565 using PCFOLD 4.0 software. (a) Predictive secondary structure at 20 °C in which four of six bases are base paired (nucleotides in hatched box). (b) Predictive secondary structure at 40 °C in which all six bases are in the loop (nucleotides in hatched boxes).

RNA dimerization kinetics indicated that the variations in dimerization yield at temperatures <50 °C were controlled by the incubation temperature (Figure 5), and did not depend upon RNA concentration (not shown). We conclude that only a subset of the monomeric RNA was under a conformation suitable for dimerization. Similar observations were reported for HIV-1 RNA dimerization (Marquet et al., 1994). A theoretical fold of PSI RNA as a function of temperature predicts two temperature-dependent structures of the 278−309 sequence (Figure 7). At 40 °C, the stem−loop is closed by the six-base loop UAGCUA (Figure 7b), while at 20 °C, four of these residues are base paired (Figure 7a). Both structures 7a and 7b were proposed by Tounekti et al. (1992) based on chemical probing of monomeric and dimeric PSI RNA *in vitro*. A third monomeric RNA structure was proposed by these authors. Although this alternative conformation for the 278−309 region is possible, it is less energetically favored (Table 2) and does not appear among the theoretical folds.

The autocomplementary UAGCUA loop of structure 7b could trigger dimer formation through loop−loop recognition. Since temperature modulates the relative amounts of species 7a and 7b, the transition seen in Figure 5 is readily rationalized. Together with our predecessors (Roy et al., 1990; Tounekti et al., 1992), we propose the following dimerization process:

$$(x)\mathrm{M} \rightarrow (x-y)\mathrm{M} + (y)\mathrm{M}^*$$

$$(x-y)\mathrm{M} + (y)\mathrm{M}^* \rightarrow (y/2)\mathrm{D} + (x-y)\mathrm{M}$$

where x and y represent the concentrations of monomeric RNAs with an unfavorable (Figure 7a) or favorable (Figure 7b) conformation, respectively.

For temperatures significantly lower than its T_m (t < 50 °C), the dimer, once formed, could be irreversible and the total amount of dimer a function of the distribution of the M and M* conformations. Increasing the temperature could induce a change in the distribution of RNA monomers (M)

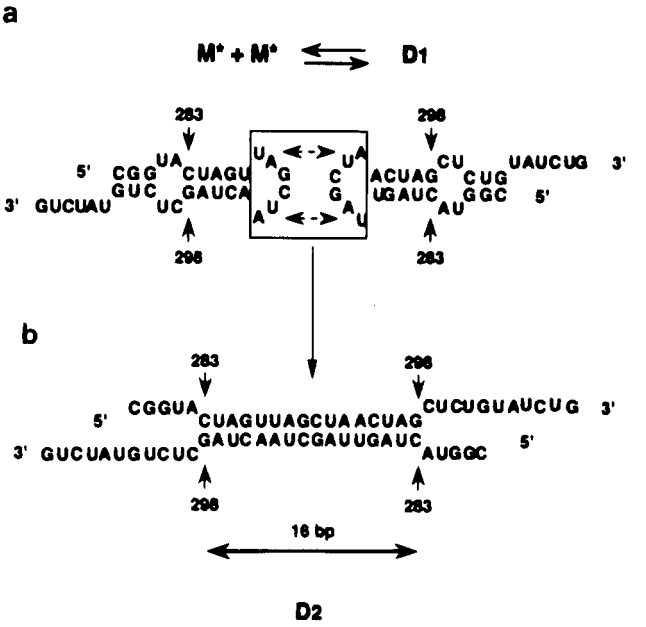

FIGURE 8: Model of the loop−loop interaction between RNA monomers giving rise to a stable dimer. Two monomers M* interact via the autocomplementary sequence UAGCUA (symbolizes by two arrows inside the box), forming an unstable dimer D1. Opening of each stem−loop leads to a more stable dimer D2 through the formation of a short RNA duplex involving a perfect annealing on 16 canonical Watson−Crick base pairs. Numbering is in relation to the cap site (+1).

and (M*) toward the more favorable conformation M* to a greater amount of dimer (D).

The overall rate of dimer formation, which is about 1000 times slower than for short complementary RNAs whose binding is controlled by diffusion, implies an additional step involving a conformational rearrangement. This is in agreement with the results obtained for a 755 nt RNA transcript of MoMuLV whose rate constant of dimerization was 250 M^{-1} s^{-1} at 37 °C (Roy et al., 1990). This leads us to postulate that the interaction between two UAGCUA (in accordance with the thermodynamic fold) or two AGCU [in accordance with the chemical probing experiments of Tounekti et al. (1992)] sequences formed an unstable dimer (D1) (Figure 8a). D1 is then converted, through the opening of the 283−298 stem−loop, into a double-stranded region *via* Watson−Crick base pairing to form a stable dimer (D2) involving 16 bp, as shown in Figure 8b.

Dimerization of MoMuLV RNA can be described as at least a three-step process: (1) a temperature-dependent intramolecular process (M → M*) leading to a "dimerizable" conformation; (2) the interaction of two monomers (M* + M* ⇔ D1) through the UAGCUA or the AGCU sequence, producing an unstable dimer D1; and (3) the evolution of D1 toward a stable dimer D2 (D1 → D2). Both the first and third steps, which imply conformational rearrangements, could correspond to the rate-limiting step. We make the *ad*

Table 2: Free Energy of Stem−Loops 278−303, Described in Figure 7, as a Function of Temperature[a]

	4 °C	10 °C	20 °C	25 °C	30 °C	35 °C	40 °C	50 °C
$\Delta G°$(a) (kcal/mol)	−13.9 (−11)	−12 (−9.7)	−8.6 (−7.1)	−6.8 (−6.0)	−5.4 (−4.9)	−3.8 (−4.1)	−2.3 (−2.6)	−0.3 (−1.1)
$\Delta G°$(b) (kcal/mol)	−8.3	−7.4	−5.9	−5.3	−4.6	−3.8	−3.1	−1.8

[a] $\Delta G°$(a) and $\Delta G°$(b) are determined by PCFOLD 4.0 software according to thermodynamic parameters of Turner et al. (1987). $\Delta G°$(a) and $\Delta G°$(b) refer to the stem−loops shown in Figure 7a and Figure 7b, respectively. Numbers in parentheses are determined from the third structure of the monomeric RNA which was proposed by Tounekti et al. (1992).

Table 3: Thermodynamic Parameters of RNA Dimer Dissociation in 100 mM NaCl[a]

	f215−565	f215−364	f237−364	f268−364	f1−725
$\Delta H°$ (kcal/mol)	(−192 ± 12) −135 ± 15	−137 ± 16	−121 ± 31	−102 ± 10	(−208 ± 14)
$\Delta S°$ [cal/(mol·K)]	(−551 ± 68) −377 ± 19	−387 ± 20	−339 ± 17	−278 ± 14	(−600 ± 41)
$\Delta G°_{37°C}$ (kcal/mol)	(−21 ± 18) −18 ± 18	−17 ± 17	−16 ± 36	−16 ± 15	(−22 ± 19)

[a] Thermodynamic parameters were determined from the plots of $1/T_m$ versus log C_t where C_t is the total RNA strand concentration. Numbers in parentheses were obtained by Roy et al. (1990). Experimental conditions are described under Materials and Methods.

hoc assumption that the third step is the rate-limiting step.

An analogous mechanism was extensively studied in the case of the control of ColE1 plasmid replication [for a review, see Eguchi et al. (1991)]. ColE1 plasmid replication is regulated by the interaction of two RNAs, *RNA I* and *RNA II*. Binding of *RNA I* to *RNA II* involves the recognition of complementary loops, which give rise to a stable complex. Eguchi et al. (1991) described the overall process as (1) a fast process implicating reversible loop−loop interaction and (2) a slow process, requiring simultaneous melting of complementary stems for the progression of hybridization.

Our model implies that the stability of D2 arose from the annealing of two complementary 283−298 sequences through Watson−Crick base pairing. Taking into account thermodynamic parameters for the prediction of RNA duplex stability determined by Freier et al. (1986), we predict enthalpy and entropy changes of −126 ± 6 kcal/mol and −342 ± 17 cal/(mol·K), respectively ($\Delta G°_{37°C}$ = −20 ± 8 kcal/mol) during formation of D2. The agreement between these theoretical values and our experimental values [−124 ± 16 kcal/mol and −346 ± 50 cal/(mol·K), corresponding to $\Delta G°_{37°C}$ = −17 ± 18 kcal/mol] derived from a determination of T_m as a function of RNA concentration for each transcript (Table 3) is consistent with the hypothesis that the thermal stability of f215−565, f215−364, f237−364, and f268−364 RNA dimers was due to duplex formation of the 283−298 autocomplementary sequence.

The rate constant for duplex formation by autocomplementary oligonucleotides decreases with increasing temperature, which leads to negative values (between −3 and −6 kcal/mol) for the activation energy, E_a (Craig et al., 1971; Pörschke & Eigen, 1971; Pörschke et al., 1973). On the other hand, a positive value suggests that intramolecular base pairing of the recognition loop interferes with duplex formation (Craig et al., 1971; Williams et al., 1989; Marquis Gacy & McMurray, 1994).

We observe positive values for each RNA transcript (Table 1) with a mean E_a value of 15.5 ± 0.5 kcal/mol. This support the idea that RNA structure, and we make the assumption *via* the stem−loop spanning nucleotides 278−309, interferes at the time of RNA dimer formation. Furthermore, the rate constant values determined for each RNA transcript revealed that there was no correlation between the RNA length and its ability to dimerize (Figure 6). Nevertheless, as f215−565 dimerized more efficiently than other RNA transcripts, structural elements localized in 215−268 and/or 364−565 sequences might favor the overall process of dimerization.

Frank-Kamenetskii (1971), based on the data of Owen et al. (1969), derived a linear relation between the T_m of natural DNA and Na^+ concentration (in the range of 0.005−0.3 M) which takes into account the fractional GC content (F_{GC}): $d(T_m)/d(\log [Na^+]) = 18.30 - 7.04F_{GC}$.

The entire 283−298 sequence has a 37.5% GC content (Figure 8b). This leads to a $d(T_m)/d(\log [Na^+])$ value of 15.6 compared to a value of 14.4 ± 0.5 in our experimental conditions (Table 4). Furthermore, Roy et al. (1990) obtained a $d(T_m)/d(\log [Na^+])$ value of 15 for the 755 nt RNA dimer. Thus, the nucleotide composition of the 283−298 autocomplementary sequence can explain the stability of our RNA dimers.

Table 4: Variation of RNA Dimer Melting Temperature (T_m) as a Function of Salt Concentration (Na^+)[a]

	$d(T_m)/d(\log [Na^+])$
f215−565	14.6 ± 1.9
f215−364	14.8 ± 1.8
f237−364	14.5 ± 1.3
f268−364	13.6 ± 1.6

[a] These values were derived from linear regression of the plots of T_m versus log [Na^+].

The last relevant point concerns the hypothetical implication of PuGGAPuA consensus sequences in the dimerization process through quartet formation involving both adenine(s) and guanine(s) [for a review, see Guschlbauer et al. (1990)]. This model was first proposed by Marquet et al. (1991) and later supported by Sundquist and Heaphy (1993) and by Awang and Sen (1993), who provided evidence that interstrand quadruplex formation is relevant to the generation of HIV-1 RNA dimer. Marquet et al. (1991) observed that a purine consensus sequence, PuGGAPuA, is found twice in the putative DLS of MoMuLV RNA at positions 359−364 and 476−481. The facts that oligonucleotide OL275−291, which was complementary to the 275−291 sequence of MoMuLV RNA, inhibited f215−565 dimerization or that f215−565Δ290−299 was unable to dimerize suggest that PuGGAPuA sequences were not involved in dimer formation of MoMuLV RNA transcripts in low ionic strength (i.e., 100 mM NaCl). Several other reports do not support involvement of the purine quartet in RNA dimerization of HIV-1_{LAI} (Laughrea & Jetté, 1994; Muriaux et al., 1995), HIV-1_{HXB2} (Fu et al., 1994), or HIV-2_{ROD} (Berkhout et al., 1993).

Chemical probing of the monomeric and dimeric PSI domain indicated that some nucleotides in the 283−298 region became less reactive upon dimerization (Tounekti et al., 1992). This was interpreted as the result of intermolecular interactions and/or intramolecular conformational rearrangements. However, Tounekti et al. (1992) concluded that the stability of the dimer is unlikely to depend only on Watson−Crick interactions, because of the following:

(1) Antisense RNA (567 to −30) is unable to dimerize. In our model (Figure 8), the hairpin structure should lead to detectable dimer due to the persistence of autocomplementary sequence in antisense RNA. To explain this discrepancy, we propose that this "undimerizable" structure in antisense RNA corresponds to a stem−loop whose theorical free energy ($\Delta G°_{37°C}$ = −4.5 kcal/mol) is higher than the one calculated for sense RNA ($\Delta G°_{37°C}$ = −3.6 kcal/mol) resulting in a stabilization of the stem. Accordingly, loop−

loop interactions would still occur in antisense RNA but would not lead to opening of the stem. In this case, only unstable dimer D1 would be formed. Another explanation, as suggested by Tounekti et al. (1992), could be that the dimerization elements have different conformations in sense and antisense RNA.

(2) The partial stability of the dimer in urea−formamide is incompatible with sole Watson−Crick interactions (more than 50% dimer is still present in 2.9 M urea and 37% formamide). These experiments were done with RNAs spanning nucleotides 1−725 (referred to as RNA 1−725). RNA dimers were preformed in 300 mM KCl and 5 mM $MgCl_2$ and then submitted to various concentrations of urea−formamide. We have conducted the same kind of experiments, as described by Tounekti et al. (1992), with f215−565 in 100 mM NaCl or in 300 mM KCl and 5 mM $MgCl_2$. We observe that if no dimer is present in up to 2.9 M urea and 37% formamide in low ionic strength, around 50% dimer is still present in high ionic strength (not shown). Furthermore, as shown by Pinder et al. (1974), very stable structures and two-stranded RNA do not melt spontaneously in moist formamide but do so on warming. Thus, we postulate that dimer stability could involve at least two different kinds of interactions under high salt concentration: Watson−Crick base pairing (corresponding to the model proposed in this work) and tertiary structure stabilization by Mg^{2+} (Laing et al., 1994; Laing & Draper, 1994) and/or formation of a purine quartet [which is stabilized by K^+; for a review, see Guschelbauer et al. (1990)].

(3) Electron micrographs do not support antiparallel association of the two RNA strands. The resolution of the published electron micrographs (Bender & Davidson, 1976; Bender et al., 1978; Kung et al., 1976; Murti et al., 1981) is insufficient to discriminate between a local parallel interaction and folding that leads to an apparent parallel orientation of the two RNA strands. In fact, some pictures indicate an antiparallel orientation of the strands (Bender & Davidson, 1976; Murti et al., 1981).

(4) Formation of heterodimers between RNA transcript 311−612 of HIV-1_{MAL} and RNA transcript 1−725 of MoMuLV was observed (Marquet et al., 1991). This cannot be easily explained by our model due to a lack of complementary between MoMuLV and HIV-1_{MAL} RNA. Again, these experiments were performed at high ionic strength (i.e., 300 mM KCl and 5 mM $MgCl_2$): thus, tertiary structure and/or formation of a purine quartet could favor interactions between HIV-1_{MAL} and MoMuLV RNA transcripts.

The mechanism of dimerization we propose is centered on the sequence (5′)C^{283}UA...UAG^{298}(3′). It is interesting to note that the 283−298 region is remarkably conserved in murine retroviruses (Tounekti et al., 1992; Konings et al., 1992). Recent reports are in accordance with this overall process. HIV-1_{MAL} RNA dimerization requires a palindromic sequence (G^{274}UGCAC^{279}) located in a hairpin loop and is triggered by a loop−loop interaction between two RNA monomers (Skripkin et al., 1994; Paillart et al., 1994). With HIV-1_{LAI}, Laughrea and Jetté (1994) and Muriaux et al. (1995) showed that a similar palindromic sequence was implicated in RNA dimer formation. Furthermore, Harrison et al. (1992) suggested potentiel base pairing across a stem−loop (loop IId) which is well conserved inside 18 HIV-1 strains.

These results could mean that the mechanisms of dimerization of MoMuLV RNA, HIV-1 RNA, and perhaps all other retroviral RNAs share the common feature of recognition of complementary nucleotides located in a hairpin loop, insofar as the sequence is accessible.

ACKNOWLEDGMENT

We thank M. Mougel for suggestions concerning this report. Thanks are due to J.-L. Darlix (ENS, Lyon), B. and C. Ehresmann (IBMC, Strasbourg), and P. Fossé (IGR, Villejuif) for helpful discussions. We are specially grateful to one of the reviewers for his/her detailed and constructive criticisms. Eric. J. Kremer and Lorna S^t Ange are acknowledged for their critical reading of the manuscript, Bernard Klonjkowski for his fruitful advice, and Anne Jullien for her technical assistance.

REFERENCES

Adam, M., & Miller, A. D. (1988) *J. Virol. 62*, 3802−3806.
Aldovini, A., & Young, R. A. (1990) *J. Virol. 64*, 1920−1926.
Armentao, D., Yu, S. F., Kantoff, P. W., Von Ruden, T., Anderson, W. F., & Gioboa, E. (1987) *J. Virol. 61*, 71−80.
Aronoff, R., & Linial, M. L. (1991) *J. Virol. 65*, 71−80.
Awang, G., & Sen, D. (1993) *Biochemistry 32*, 11453−11457.
Bender, M. A., Palmer, T. D., Gelinas, R. E., & Miller, D. (1987) *J. Virol. 61*, 1639−1646.
Bender, W., & Davidson, N. (1976) *Cell 7*, 595−607.
Bender, W., Chien, Y.-H., Chattopadhyay, S., Vogt, P. K., Gardner, M. B., & Davidson, N. (1978) *J. Virol. 25*, 888−896.
Berkhout, B., Oude Essink, B. B., & Schoneveld, I. (1993) *FASEB J. 7*, 181−187.
Bieth, E., Gabus, C., & Darlix, J.-L. (1990) *Nucleic Acids Res. 18*, 119−127.
Coffin, J. M. (1984) in *RNA Tumour Viruses* (Weiss, R., Teich, N., Varmus, H., & Coffin, G., Eds.) Vol. 1, pp 261−368, Cold Spring Harbor Laboratory Press, Cold Spring Harbor, NY.
Craig, M. E., Crothers, D. M., & Doty, P. (1971) *J. Mol. Biol. 62*, 383−401.
Darlix, J.-L., Gabus, C., Nugeyre, M. T., Clavel, F., & Barré-Sinoussi, F. (1990) *J. Mol. Biol. 216*, 689−699.
Eguchi, Y., Itoh, T., & Tomizawa, J.-I. (1991) *Annu. Rev. Biochem. 60*, 631−652.
Frank-Kamenetskii, M. D. (1971) *Biopolymers 10*, 2623−2624.
Freier, S. M., Kiersek, R., Jaeger, J. A., Sugimoto, N., Caruther, M. H., Neilson, T., & Turner, D. H. (1986) *Proc. Natl. Acad. Sci. U.S.A. 83*, 9373−9377.
Fu, W., Gorelick, R. J., & Rein, A. (1994) *J. Virol. 68*, 5013−5018.
Grosjean, H., Söll, D. G., & Crothers, D. M. (1976) *J. Mol. Biol. 103*, 499−519.
Guschlbauer, W., Chantot, J.-F., & Thiele, D. (1990) *J. Biomol. Struct. Dyn. 8*, 491−511.
Harrison, G. P., & Lever, A. M. L. (1992) *J. Virol. 66*, 4144−4153.
Haseltine, W. A., Maxam, A. M., & Gilbert, W. (1977) *Proc. Natl. Acad. Sci. U.S.A. 74*, 989−993.
Hu, W.-S., & Temin, H. M. (1990) *Proc. Natl. Acad. Sci. U.S.A. 87*, 1556−1560.
Katz, R. A., Terry, R. W., & Skalka, A.-M. (1986) *J. Virol. 59*, 163−167.
Konings, D. A. M., Nash, M. A., Maizel, J. V., & Arlinghaus, R. B. (1992) *J. Virol. 66*, 632−640.
Kung, H.-J., Bender, W., Bailey, J. M., Davidson, N., Nicolson, M. O., & McAllister, R. M. (1976) *Cell 7*, 609−620.
Labuda, D., & Pörschke, D. (1980) *Biochemistry 19*, 3799−3805.
Laing, L. G., & Draper, D. E. (1994) *J. Mol. Biol. 237*, 560−576.
Laing, L. G., Gluick, T. C., & Draper, D. E. (1994) *J. Mol. Biol. 237*, 577−587.
Laughrea, M., & Jetté, L. (1994) *Biochemistry 33*, 13464−13474.

Leis, J., Baltimore, D., Bishop, J. M., Coffin, J., Fleissner, E., Goff, S. P., Orozlan, S., Robinson, H., Skalka, A. M., Temin, H. M., & Vogt, V. (1988) *J. Virol. 62*, 1808−1809.
Lever, A., Gottlinger, H., Haseltine, W., & Sodroski, J. (1989) *J. Virol. 63*, 4085−4087.
Linial, M. L., & Miller, A. D. (1990) *Curr. Top. Microbiol. Immunol. 157*, 125−152.
Luo, G., & Taylor, J. (1990) *J. Virol. 64*, 4321−4328.
Mann, R., & Baltimore, D. (1985) *J. Virol. 54*, 401−407.
Mann, R., Mulligan, R. C., & Baltimore, D. (1983) *Cell 33*, 153−159.
Marquet, R., Baudin, F., Gabus, C., Darlix, J.-L., Mougel, M., Ehresmann, C., & Ehresmann, B. (1991) *Nucleic Acids Res. 19*, 2349−2357.
Marquet, R., Paillart, J.-C., Skripkin, E., Ehresmann, C., & Ehresmann, B. (1994) *Nucleic Acids Res. 22*, 145−151.
Marquis Gacy, A., & McMurray, C. T. (1994) *Biochemistry 33*, 11951−11959.
Moore, J. W., & Pearson, R. G. (1981) in *Kinetics and Mechanisms* (John Wiley & Sons, Eds.) 3rd ed., Wiley-Interscience, New York.
Muriaux, D., Girard, P.-M., Bonnet-Mathonière, B., & Paoletti, J. (1995) *J. Biol. Chem.* (in press).
Murphy, J. E., & Goff, S. P. (1989) *J. Virol. 63*, 319−327.
Murti, K. G., Bondurant, M., & Tereba, A. (1981) *J. Virol. 37*, 411−419.
Owen, R. J., Hill, L. R., & Lapage, S. P. (1969) *Biopolymers 7*, 503−516.
Paillart, J.-C., Marquet, R., Skripkin, E., Ehresmann, B., & Ehresmann, C. (1994) *J. Biol. Chem. 269*, 27486−27493.
Panganiban, A. T., & Fiore, D. (1990) *Science 241*, 1064−1069.
Petersheim, M., & Turner, D. H. (1983) *Biochemistry 22*, 256−263.
Pinder, J. C., Staynov, D. Z., & Gratzer, W. B. (1974) *Biochemistry 13*, 5367−5373.
Pörschke, D., & Eigen, M. (1971) *J. Mol. Biol. 62*, 361−381.
Pörschke, D., Uhlenbeck, O. C., & Martin, F. H. (1973) *Biopolymers 12*, 1313−1335.
Prats, A.-C., Sarih, L., Gabus, C., Litvak, S., Keith, G., & Darlix, J.-L. (1988) *EMBO J. 7*, 1777−1783.
Prats, A.-C., Roy, C., Wang, P., Erard, M., Housset, V., Gabus, C., Paoletti, C., & Darlix, J.-L. (1990) *J. Virol. 64*, 774−793.
Rein, A. (1994) *Arch. Virol., Suppl. 9*, 519−522.
Roy, C., Tounekti, N., Mougel, M., Darlix, J.-L., Paoletti, C., Ehresmann, C., Ehresmann, B., & Paoletti, J. (1990) *Nucleic Acids Res. 18*, 7287−7292.
Sambrook, J., Fritch, E. F., & Maniatis, T. (1989) in *Molecular Cloning: A Laboratory Manual* (Nolan, C., Ed.) 2nd ed., Cold Spring Harbor Laboratory Press, Cold Spring Harbor, NY.
Shinnick, T. M., Lerner, R. A., & Sutcliffe, J. G. (1981) *Nature 293*, 543−548.
Skripkin, E., Paillart, J.-C., Marquet, R., Ehresmann, B., & Ehresmann, C. (1994) *Proc. Natl. Acad. Sci. U.S.A. 91*, 4945−4949.
Stocker, A. W., & Bissel, M. J. (1979) *J. Virol. 62*, 3802−3806.
Sundquist, W. I., & Heaphy, S. (1993) *Proc. Natl. Acad. Sci. U.S.A. 90*, 3393−3397.
Temin, H. M. (1991) *Trends Genetics 7*, 71−74.
Torrent, C., Bordet, T., & Darlix, J.-L. (1994) *J. Mol. Biol. 240*, 434−444.
Tounekti, N., Mougel, M., Roy, C., Marquet, R., Darlix, J.-L., Paoletti, J., Ehresmann, B., & Ehresmann, C. (1992) *J. Mol. Biol. 223*, 205−220.
Turner, D. H., Sugimoto, N., Jaeger, J. A., Longfellow, C. E., Freier, S. M., & Kiersek, R. (1987) *Cold Spring Harbor Symp. Quant. Biol. 52*, 123−133.
Watanabe, S., & Temin, H. M. (1982) *Proc. Natl. Acad. Sci. U.S.A. 79*, 5986−5990.
Weiss, R. A., Mason, W. S., & Vogt, P. K. (1973) *Virology 52*, 535−552.
Williams, A. P., Longfellow, C. E., Freier, S. M., Kiersek, R., & Turner, D. H. (1989) *Biochemistry 28*, 4283−4291.

BI950025O